

# Electron Acceleration in Carbon Nanotubes

## The Next Generation LWFA

C. Bonțoiu<sup>1</sup>, Ö. Apsimon<sup>2</sup>, L. Bandiera<sup>3</sup>, A. Bonatto<sup>4</sup>, G. Cavoto<sup>5</sup>, I. Drebot<sup>6</sup>, B. Lei<sup>1</sup>, J. Resta-López<sup>7</sup>, P. Martín-Luna<sup>7</sup>,  
J. Rodríguez Pérez<sup>8</sup>, A. Sytov<sup>3</sup>, C. Valagiannop<sup>9</sup>, C. Welsch<sup>1</sup>, G. Xia<sup>2</sup>

<sup>1</sup>Univ. of Liverpool, Dep. of Physics, Liverpool, United Kingdom, <sup>2</sup>Univ. of Manchester, Dep. of Physics, Manchester, United Kingdom

<sup>3</sup>I.N.F.N., Ferrara, Italy, <sup>4</sup>Fed. Univ. of Health Sciences, Dep. of Social and Applied Sciences, Porto Alegre, Brazil,

<sup>5</sup>Sapienza University, Dep. of Physics, Rome, Italy, <sup>6</sup>I.N.F.N., Milan, Italy, <sup>7</sup>Univ. Valencia, Instituto de Física Corpuscular, Paterna, Spain

<sup>8</sup>Univ. Valencia, Institute of Materials Science, Paterna, Spain, <sup>9</sup>Nat. Technical Univ. of Athens, School of Electrical and Computer Eng., Athens, Greece

### Abstract

We report the first numerical demonstration of electron self-injection and resonant acceleration in ordered Carbon Nanotube (CNT) structures. Using the PIconGPU code [1] CNT bundles are modelled as 25 nm-thick carbon tubes of  $10^{22}$  cm<sup>-3</sup> plasma density. Following their ionization with 3-cycles-long laser pulse of 800 nm wavelength and  $10^{21}$  W cm<sup>-2</sup> peak intensity, laser wakefield acceleration (LWFA) [2] is triggered in the resulting carbon plasma with an effective density of  $10^{20}$  cm<sup>-3</sup>. Simulation results indicate that self-injected fs-long electron bunches with hundreds of pC charge can be accelerated at gradients which exceed 1 TeV/m. Both charge and accelerating gradient figures are unprecedented when compared with LWFA in gaseous plasma [3].

### Introduction

While LWFA research is currently dominated by meticulously tailored gaseous targets [3], solid-state plasmas may soon become an alternative, due to their inherent advantages such as higher electron density and wider topological flexibility. It is possible for example to prepare hollow targets with controllable effective plasma density. Carbon nanomaterials such as graphene [4] and CNTs are good candidates due to the recent progress in their manufacturing techniques. This work considers 25 nm-thick bundles (ropes) of CNTs [5] rather than large volumes (forests) of densely packed CNTs. Considering that a CNT bundle may contain tens or hundreds of tubes and inherent voids, it is reasonable to assume that the density of atoms is in the order of  $10^{22}$  cm<sup>-3</sup>. A target can be manufactured distributing CNT bundles in concentric shells, as shown in **Figure 1**, with an effective plasma density of  $10^{20}$  cm<sup>-3</sup>.

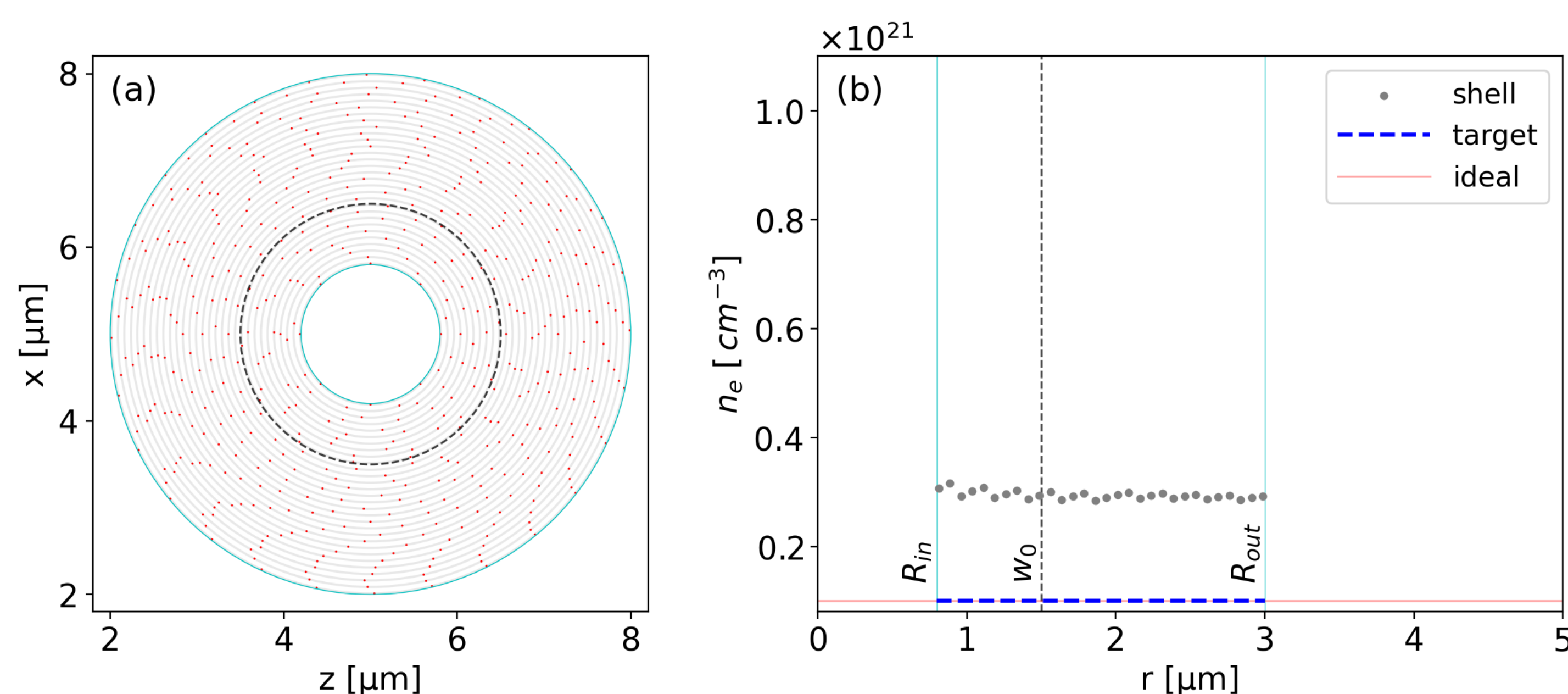


**Figure 1** – (a) Transverse view of a CNT target made of 535 bundles, grouped in 30 shells with a 50 nm gap; (b) The corresponding plasma density for each shell and for the whole target. The black dashed circle indicates the laser spot size.

This is a good choice for a 800 nm – wavelength laser pulse, since the ratio of the plasma frequency to the laser frequency indicates an underdense interaction. For comparison, **Table 1** shows why effective plasma density orders of  $10^{21}$  cm<sup>-3</sup> and  $10^{22}$  cm<sup>-3</sup> cannot be used, effectively ruling out bulk CNT targets.

Parameter	Target			Laser	Unit
Plasma density, $n_e$	$10^{20}$	$10^{21}$	$10^{22}$	-	cm <sup>-3</sup>
Angular Frequency	$\omega_p = 0.564$	$\omega_p = 1.784$	$\omega_p = 5.641$	$\omega_0 = 2.355$	$\times 10^3$ rad-THz
$\omega_p/\omega_0$	0.240	0.758	2.396	-	-
Wavelength	$\lambda_p = 3.339$	$\lambda_p = 1.056$	$\lambda_p = 0.334$	$\lambda = 0.800$	μm
$(\lambda/\lambda_p)^2$	$5.741 \times 10^{-2}$	$5.741 \times 10^{-1}$	5.741	-	-

**Table 1** – Effective plasma density parameters versus laser parameters.

The target bore is an important feature and plays the same role as the shortly-lived plasma channels [6] produced in gaseous targets. Here its radius is roughly half of the laser spot size. The bore guides the laser pulse along several Rayleigh lengths and simultaneously provides the ions lattice along which the electron bunch is accelerated. In this example simulations were done using the laser parameters

Parameter	Value	Unit
Wavelength, $\lambda$	800	nm
Period, T	2.66	fs
Energy, E	301	mJ
Peak Intensity, $I_0$	$10^{21}$	W/cm <sup>2</sup>
Potential vector, $a_0$	21.6	-
Pulse Length, $\Delta t$	8	fs
Spot Size, $w_0$	1.5	μm

**Table 2** – Laser parameters.

shown in **Table 2**. In addition, it is worth mentioning that the self-injection and acceleration scheme also works for larger values of the spot size  $w_0$ , as long as the ratio to the bore radius is kept to a value of about 2. Here the choice is motivated by the computational limitations. Similarly, the full pulse length  $\Delta t$  represents 3 laser cycles, but slightly longer pulses can be used. On the contrary, only peak intensity values in the order  $10^{21}$  W/cm<sup>2</sup> lead to significant target ionization and consequently electron self-injection and resonant acceleration.

### Numerical Results

The laser pulse ionizes the interaction region, repelling electrons towards the outer shells, generating a moving wakefield bubble. As shown in **Figure 2**, Electrons are then self-injected at the back of the bubble and experience TV/m longitudinal electric fields. In this example an electron bunch of 830 pC charge is resonantly accelerated to about 28 MeV in 15 μm. The acceleration gradient is 1.87 TeV/m (!).

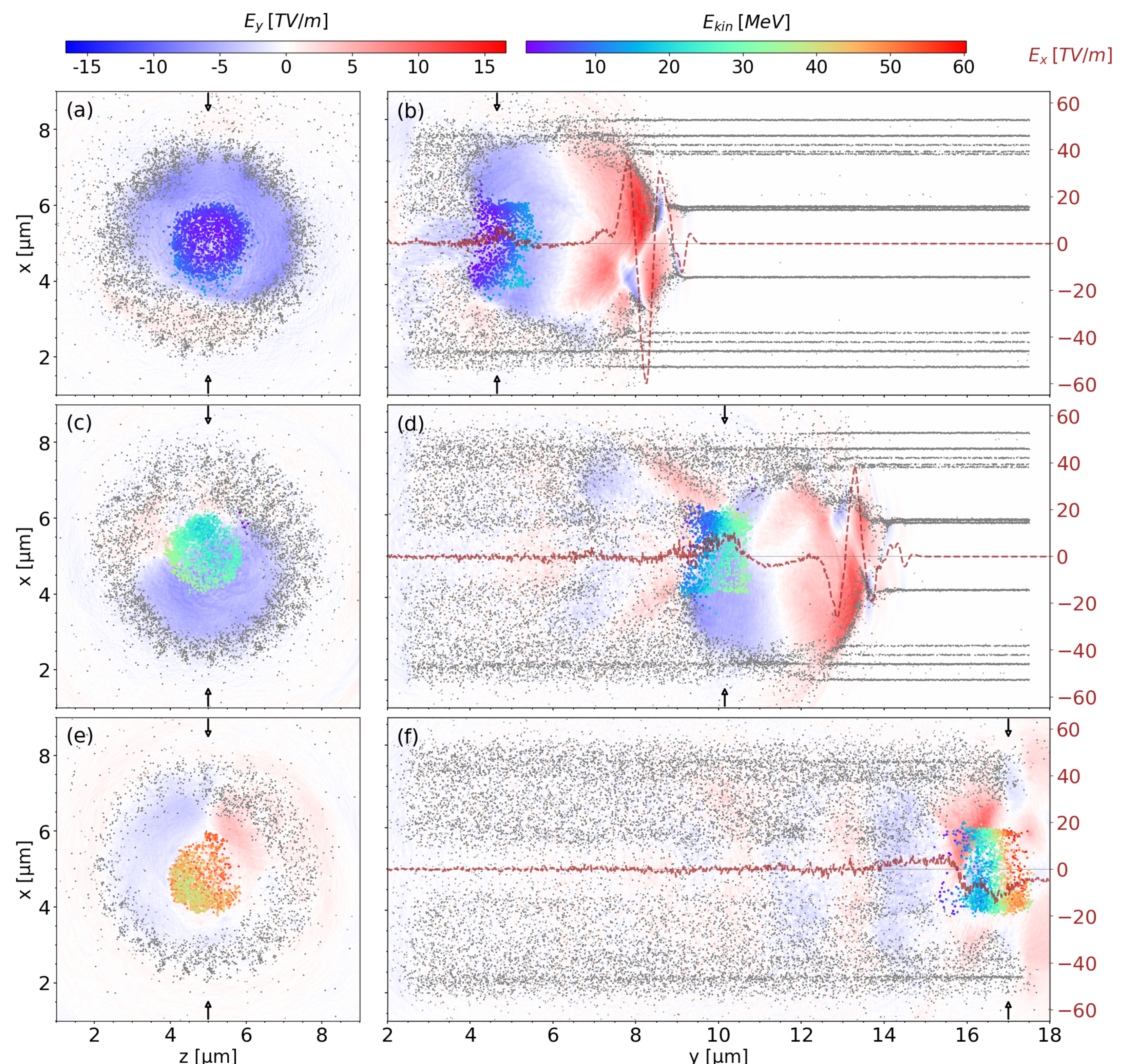


**Figure 2** – Electron macroparticles shown as gray dots and the longitudinal electric field shown as a colour density plot: (a-b)  $t/T = 11$ ; (c-d)  $t/T = 18$ ; (e-f)  $t/T = 25$ .

As shown in **Figure 3**, the acceleration scheme yields large energy spread and divergence. Solutions to mitigate them are sought by introducing a radial gradient for the plasma density since this parameter directly decides the laser phase velocity to which the electron bunch needs to be matched.

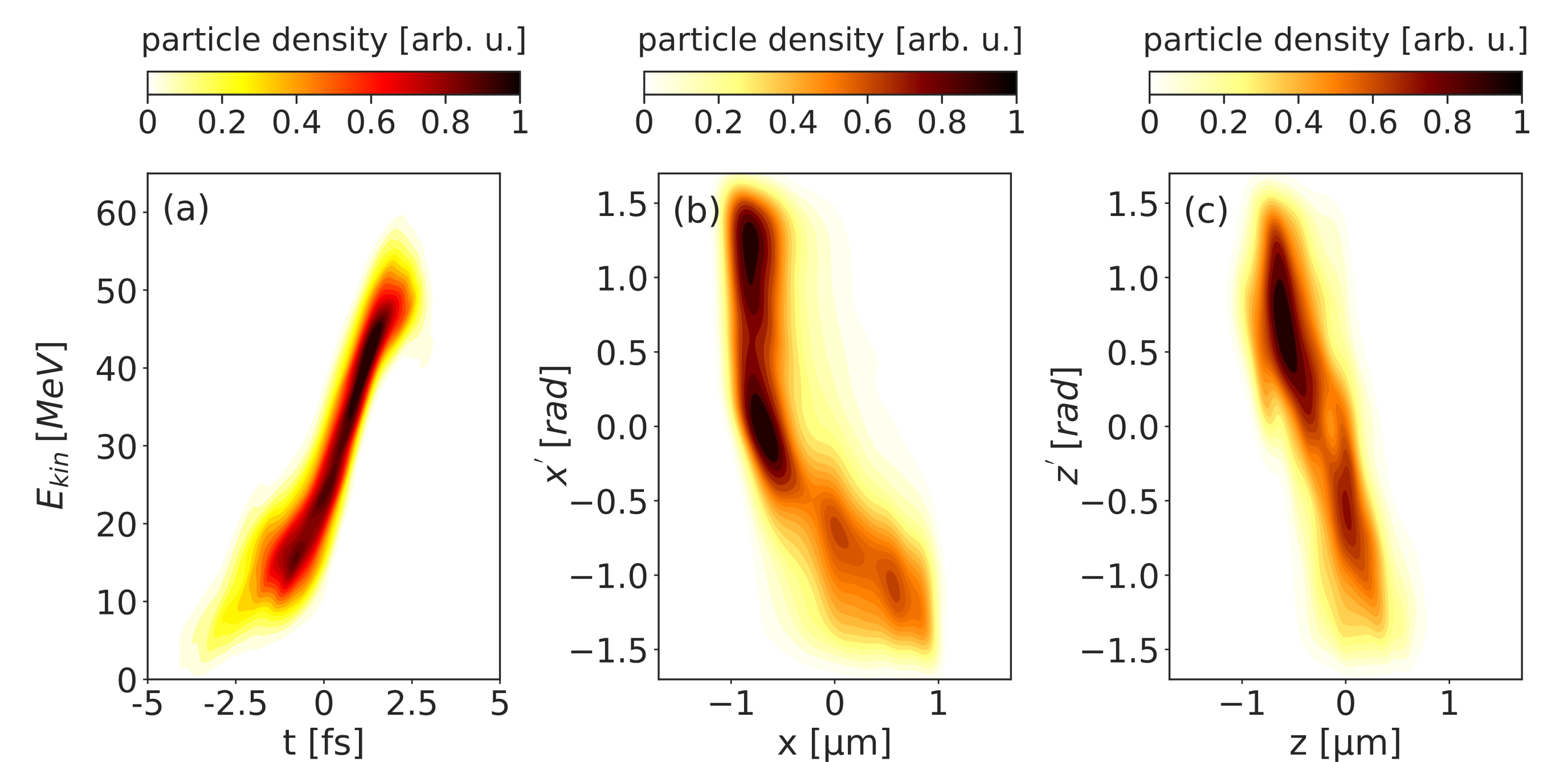


**Figure 3** – Bunch phase space at extraction ( $t/T = 25$ ): (a) Longitudinal phase space; (b) Vertical phase space; (c) Horizontal phase space.

### Conclusions

The collaboration is currently preparing optimal targets for a proof-of-principle experiment, investigating manufacturing techniques. Should this experiment prove successful, the concept presented in the current work may offer a novel alternative acceleration scheme and represent the first demonstration of LWFA in a solid-state plasma.

### References

- [1] H. Bura et al., *PIconGPU: A Fully Relativistic Particle-in-Cell Code for a GPU Cluster*, IEEE Transactions on Plasma Science 38.10 (Oct. 2010), pp. 2831–2839;
- [2] E. Esarey, C. Schroeder, W. Leemans, *Physics of laser-driven plasma-based electron accelerators*, Rev. Mod. Phys. 81 (27 Sept. 2009), pp. 1229–1285;
- [3] A. Gonsalves et al., *Petawatt Laser Guiding and Electron Beam Acceleration to 8 GeV in a Laser-Heated Capillary Discharge Waveguide*, Phys. Rev. Lett. 122.8 (Feb. 2019), p. 084801;
- [4] C. Bonțoiu et al., *TeV/m catapult acceleration of electrons in graphene layers*, Scientific Reports, (2023) 13:1330;
- [5] A. Thess et al., *Crystalline Ropes of Metallic Carbon Nanotubes*, Science Vol. 273, No. 5274 (Jul. 1996), p. 483–487;
- [6] A. Picksley et al., *Guiding of high-intensity laser pulses in 100-mm-long hydrodynamic optical-field-ionized plasma channels*, Phys. Rev. Accel. Beams Vol. 23, No. 8 (Aug. 2020), p. 081303.